Processing, Properties, and Design of Advanced Ceramics and Composites II

Edited by
Narottam P. Bansal
Ricardo H. Castro
Michael Jenkins
Amit Bandyopadhyay
Susmita Bose
Amar Bhalla
J.P. Singh
Morsi M. Mahmoud
Gary Pickrell
Sylvia Johnson

Ceramic Transactions
Volume 261

The American Ceramic Society

WILEY

Processing, Properties, and Design of Advanced Ceramics and Composites II

Processing, Properties, and Design of Advanced Ceramics and Composites II

Ceramic Transactions, Volume 261

Edited by

Narottam P. Bansal
Ricardo H. R. Castro
Michael Jenkins
Amit Bandyopadhyay
Susmita Bose
Amar Bhalla
J.P. Singh
Morsi M. Mahmoud
Gary Pickrell
Sylvia Johnson

WILEY

This edition first published 2017

Registered Office
John Wiley & Sons, Inc., 111 River Street, Hoboken, NJ 07030, USA

Editorial Office
111 River Street, Hoboken, NJ 07030, USA

For details of our global editorial offices, customer services, and more information about Wiley products visit us at www.wiley.com.

Wiley also publishes its books in a variety of electronic formats and by print-on-demand. Some content that appears in standard print versions of this book may not be available in other formats.

Library of Congress Cataloging-in-Publication Data is available
ISBN: 9781119423805
ISSN: 1042-1122

Cover design by Wiley

10 9 8 7 6 5 4 3 2 1

Contents

SINTERING AND RELATED POWDER PROCESSING

SURFACE PROPERTIES OF BIOMATERIALS

INNOVATIVE PROCESSING

DIELECTRIC MATERIALS AND ELECTRONIC DEVICES

PROCESSING AND PERFORMANCE OF MATERIALS USING MICROWAVES, ELECTRIC, AND MAGNETIC FIELDS

THERMAL PROTECTION MATERIALS AND SYSTEMS

ADVANCED MATERIALS FOR HARSH ENVIRONMENTS

ZIRCONIA BASED MATERIALS

CONTROLLED SYNTHESIS, PROCESSING, AND APPLICATIONS OF STRUCTURAL AND FUNCTIONAL NANOMATERIALS

CERAMIC OPTICAL MATERIALS

MULTIFUNCTIONAL OXIDES

Preface

This volume contains 36 papers presented during the Materials Science & Technology 2016 Conference (MS&T'16), held October 23–27, 2016 at the Salt Palace Convention Center, Salt Lake City, Utah. Papers from the following symposia are included in this volume:

- Advanced Materials for Harsh Environments
- Advances in Dielectric Materials and Electronic Devices
- Advances in Ceramic Matrix Composites
- Ceramic Optical Materials
- Controlled Synthesis, Processing, and Applications of Structural and Functional Nanomaterials
- Innovative Processing and Synthesis of Ceramics, Glasses, and Composites
- International Standards for Properties and Performance of Advanced Ceramics
- Multifunctional Oxides
- Rustum Roy Memorial Symposium on Processing and Performance of Materials Using Microwaves, Electric, and Magnetic Fields
- Sintering and Related Powder Processing Science and Technology
- Surface Properties of Biomaterials
- Thermal Protection Materials and Systems
- Zirconia Based Materials for Cutting Edge Technology

These conference symposia provided a forum for scientists, engineers, and technologists to discuss and exchange state-of-the-art ideas, information, and technology on advanced methods and approaches for processing, synthesis, characterization, and applications of ceramics, glasses, and composites.

Each manuscript was peer-reviewed using The American Ceramic Society's review process. The editors wish to extend their gratitude and appreciation to all the authors for their submissions and revisions of manuscripts, to all the participants and session chairs for their time and effort, and to all the reviewers for their valuable comments and suggestions.

We hope that this volume will serve as a useful reference for the professionals

working in the field of synthesis and processing of ceramics and composites as well as their properties.

NAROTTAM P. BANSAL
RICARDO H. R. CASTRO
MICHAEL JENKINS
AMIT BANDYOPADHYAY
SUSMITA BOSE
AMAR BHALLA
J.P. SINGH
MORSI M. MAHMOUD
GARY PICKRELL
SYLVIA JOHNSON

Advances in Composites

THE EFFECT OF PASTE WATER CONTENT ON THE GREEN MICROSTRUCTURE OF EXTRUDED TITANIUM DIOXIDE

Mustafa Kanaan Alazzawi, Richard A. Haber

Department of Materials Science and Engineering, Rutgers University

Piscataway, New Jersey,08854

Keywords: TiO_2; torque rheometer; capillary rheometer; microstructure; green strength

ABSTRACT

Microstructural variability in extrudates can cause flaws and undesirable pores in the green structure. This variability influences the green strength of extrudates. Titanium dioxide is one of the most widely used in catalysts, typically used in either a pressed pellet or an extruded substrate. In this study, extruded titania was considered. Both torque and capillary rheometer analyses were studied for pastes varying water and binder content. An infiltrated technique was employed to visualize microstructural variability. In the study, mixing torque and extrusion pressure were measured. The green strength of extrudates was studied. The effect of varying the water content in the extruded TiO_2 will be shown to affect pore distribution, densification, agglomeration size, and visible microdefects. A correlation between water content, mixing torque, extrusion pressure, green strength, and green microstructure are shown.

INTRODUCTION

A wide range of products such as catalytic converters and insulators are produced using extrusion processes. Catalysts produced using TiO_2 or Al_2O_3 have applications such as oil refining and energy production[1,2]. However, the production processes can cause severe variations in the microstructure which can lead to fractures, uneven pores, and agglomerations especially in a complex system. The agglomerations can impede the active sites of catayst[3]. The batch materials typically are water, binder and micron or submicron particulates of powder all of them that form the paste. The batch materials could play an important role in determining the green strength of extruded materials and the pore volume, pore distribution, and particle arrangement of extrudates.

Previous studies have been done on the paste behavior and phase migration during the extrusion process without considering the microstructure and green strength. Rough et al (2000) claimed that the water redistribution within the paste is related to initial water content, extrusion rate and die geometry[4]. The claim is based on studying the dewatering rate, the pressure- displacement behavior, and the extrusion velocity[4]. Guilherme et al (2013) investigated three materials (porcelain, earthenware, and terracotta), the extrusion and completion test were performed and the Benbow–Bridgwater parameters were calculated. The results showed that the ability of materials to be extruded is dependent on the plasticity of these materials that related to the initial composition and processing[5].

In assessing the extrudability of a paste, common analytical methods include both torque and capillary rheometer. The torque rheometer uses to evaluate the rheological behavior of the mixture[6]. The capillary rheometer is a common means of analyzing the shear rate behavior of a paste. Here the paste is forced, under a constant speed and shear rate[7], through dies of varying geometry where the materials deform at the die entrance[4]. The challenges that are associated with the extrusion process are inhomogeneity, agglomeration, phase migration and air bubbles. The water movement in the rheometer can cause pressure variations and surface defects[8].

This research aims to understand the microstructure variations and extrusion parameters of extruded materials using TiO_2 powder and a sodium carboxymethyl cellulose (CMC) binder.

EXPERIMENTAL

In this study, G2 TiO_2 powder (Cristal Global, Paris, France) was mixed with sodium carbonoxymethyl cellulose (CMC) binder (Sigma-Aldrich, Missouri, USA), and water to form a paste as shown in Table 1. To achieve an extrudable paste, the materials were pre-mixed in the dry state then pre-mixed by in a container with a spatula with water to form a wet mixture. The wet mixture was mixed using Haake Rheocord 9000 torque rheometer (Haake Buchler, New Jersey, USA). The mixer consists of pair of sigma blades, a chute that provides ability to load the wet mixture, and a water cooling system. The water cooling system was used to mitigate the frictional heat challenge since the low temperature of mixing is important to get a homogenous and well binder- powder dispersion[9]. The temperature was monitored to keep it within a certain range (30.0-40.0) °C. The mixing time and speed were held constant at 100.0 RPM for 35.0 min to reach a degree of an acceptable mixedness. The moisture content of pre-mixing and post-mixing materials was measured to ensure that the water within the mixture and paste was constant. Figure 1 shows the typical mixing behavior using a torque rheometer showing the loading peak torque as well as steady state mixing torque. The torque of mixing is the resistance of the mixture to the shear of the rotating blades. The lower torque value indicates a deagglomerated paste[9,10].

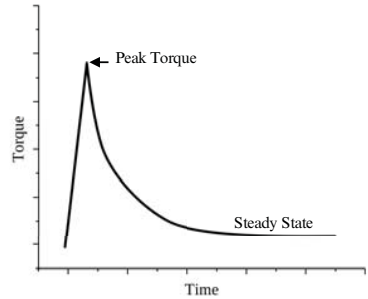

Figure 1. A typical mixing profile shows the mixing regions.

The extrusion was carried out using RH2000 capillary rheometer (Malvern Instruments Ltd, Massachusetts, USA) where the paste was extruded at 5.0mm/min which provides a constant extrusion shear rate through a cylindrical die with 8.0 mm length and 2.0 mm diameter. A typical extrusion behvior shows the compaction pressure of the paste within the barrel[11]. The paste yields at the die entrance and reaches the steady state flow. In idealized system the pressure of steady state is constant as shown in Figure 2. However, there are fluctuations in the steady state pressure because of the phase migration, water redistribution, and trapped air[11]. The extruded materials were placed in Thermolyne mechanical oven for about 24.0 hrs at 100.0 °C to ensure that the moisture was removed and the binder was not degraded.

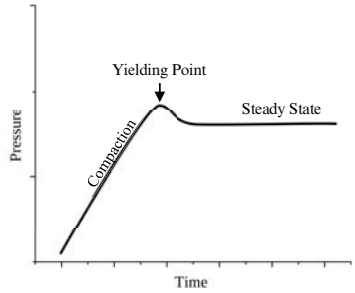

Figure 2. A typical extrusion profile shows the extrusion regions.

Table 1. Pastes composition.

CMC (%)	H_2O (%)
1.50	50.0-56.4
1.86	50.0-56.4
2.48	50.0-56.4

The green strength of dried samples was measured using Kinexus Rotational Rheometer (Malvern Instruments Ltd, Massachusetts, USA). The green strength test was run following the standard test method ASTM D6175-03[12]. Six cylindrical samples with approximately 2.0 mm diameter were selected randomly. The samples were sectioned into length between (3.0-4.0) mm to keep the length to diameter ratio equal or greater than 1:1 ratio[12]. The dried samples were placed between two flat surfaces, the top geometry (PU25) moves toward a stationary geometry (PL25) as shown in Figure 3. The force of compression test is 20.0 N to measure the strength per length. Figure 4 shows A typical green strength profile of Kinexus rotational rheometer vs the extrudate diameter dimension changes (distance). The yielding region represents the dried crush strength is the maximum value in this region.

$$x = \frac{F}{L}$$

Where:

x: The strength of samples per length (N/mm),

F: The compressive force (N),

L: The length of sample along its cylindrical axis (mm).

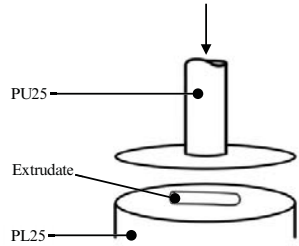

Figure 3. Schematic shows the top geometry (PU25) and the stationary geometry (PL25) of Kinexus rotational rheometer.

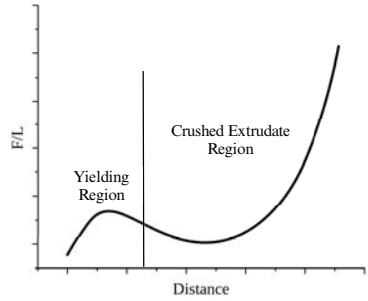

Figure 4. A typical Kinexus rotational rheometer profile for green strength measurement.

For further experiments, the binder must be removed. TGA (Thermogravimetric analysis) was conducted using the SDT Q600 (TA instruments, Delaware, USA) to determine the temperature of degradation that should be reached prior to the onset of sintering which typically begins above 750.0°C. The condition of the experiment was 10.0°C/min to 1400.0°C. The result indicates that the temperature of degradation is 650.0°C where the residual is about 23.0 wt% as shown in Figure 5. For subsequent handling all extrudates were heat treated to 650.0°C in air.

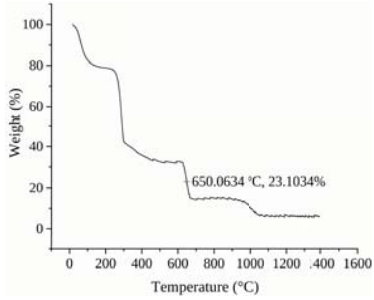

Figure 5. A degradation behavior of the binder within the extrudate.

In binder free and dry extrudates, the porous microstructure was evaluated. This is challenging as the extrudate is weak. A metallurgical epoxy was used to fill the pores and allow for polishing and examination. This epoxy in addition to providing strength to the extrudate providing contrast with the titania and other phases for scanning electron microscope (SEM) analysis. Spurr's Kit (Electron Microscopy Science, Pennsylvania, USA) was used to embed the samples following the mix formula: 23.0% of ERL 4221, 18.0% of diglycidyl ether of polypropylene glycol (DER 736), 58.0% of nonenyl succinic anhydride (NSA) and 0.693% of dimethylaminoerhanol (DMAE). The viscosity of epoxy was lowered at 60.0 °C for 15.0 min. The samples were kept under vacuum for 45.0 min to remove the bubbles that are formed within the epoxy. The infiltrated samples were cured at 70.0°C for 24.0 hrs. Infiltrated extrudates were mechanically polished using abrasive papers of 350, 600 and 1200 grits and (1.0, 0.25 and 0.05) µm diamond suspensions[13]. The samples were fixed to the SEM stubs with carbon tape and coated with silver and 15.0 nm of the gold layer to mitigate the charging issues.

The microstructure was imagined using SEM (Zeiss, Minnesota, USA). The scanning direction is from the edge toward the center of the two extrudates cross-section of each batch which were selected randomly to get a close porosity estimation as shown in Figure 6. The back scattered electron detector, 15.0kV EHT, and 60.0 µm aperture size were used. The images were analyzed using ImageJ (National Institutes of Health, Maryland, USA) to estimate the porosity variations across the cross-section of more than 650 images.

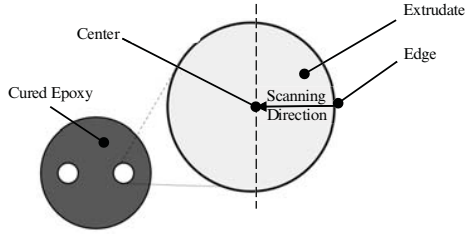

Figure 6. Schematic shows the direction of scanning from the edge toward the center of the extrudate's cross-section.

RESULTS AND DISCUSSION

Initially the effect of water content was examined to determine the optimal composition of TiO_2, binder and water mixture was determined as shown in Table1. The results represent the mixing torque, extrusion pressure, green strength, and microstructure as a function of variation in water content. A range of water content (50.0%-56.4%) was found to produce extrudates without observable surface defects. In this paper, we will consider the high water (56.4%) and the low water (50.0%) content as shown in Table 2.

Table 2. Samples terminology and composition.

Extrudate	H_2O (%)	CMC (%)	Die (L x Dia. in mm)
Low Water-Low Binder (LWLB)	50.0	1.5	8.0 x 2.0
High Water-Low Binder (HWLB)	56.4		
Low Water-High Binder (LWHB)	50.0	4.0	
High Water-High Binder (HWHB)	56.4		

MIXING RESULTS

Figure 7 below shows the peak torque of the high binder mixture is higher than the peak torque of the low binder mixture. The high water content shows a lower peak torque. The low water mixture shows a higher steady state torque and a longer time to achieve steady state. On the contrary, the high water mixture shows a lower steady state torque and a shorter time to achieve steady state. The low water content does not lead to de-agglomerated paste; hence, the agglomerated particles shows a higher resistance to the shear of the rotating blades.

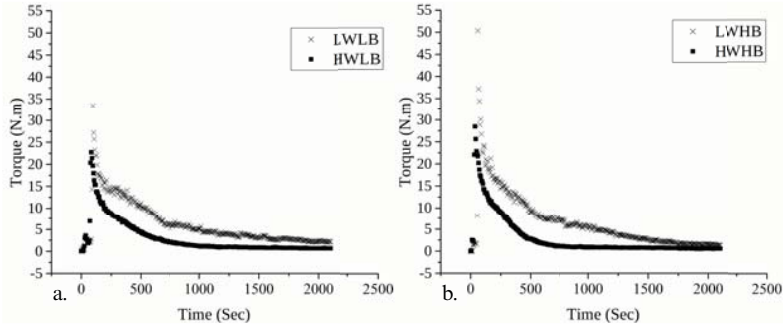

Figure 7. (a) The mixing torque of the low H_2O vs the high H_2O for the low binder mixture, (b) The mixing torque of the low H_2O vs the high H_2O for the high binder mixture.

A water range between high (56.4%) and low (50.0%) for the high and low binder mixture was investigated to study the steady state torque as shown in Figure 8. As the water content increases, the steady state torque deceases.

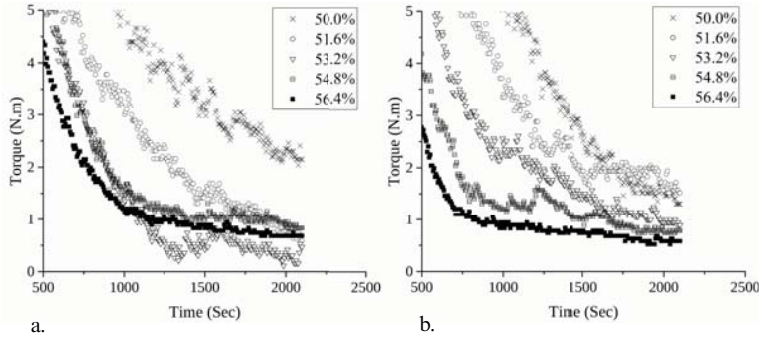

Figure 8. Mixing profiles of a water range (50.0-56.4%). (a) Low binder and, (b) High binder.

EXTRUSION RESULTS

Figure 9 shows the capillary rheomety results for the different pastes examined. The results show that the extrusion pressure of high water paste is higher than the extrusion pressure of low water paste with both low and high binder. The steady state pressure duration is longer in the high water

paste. The steady state extrusion pressure of the high water paste shows fluctuations because of phase movement and air bubbles.

The quality of the high water extrudate for high binder content was improved because there is enough water to form a thin layer of lubrication which lowered the effect of the extrusion shear along the die land.

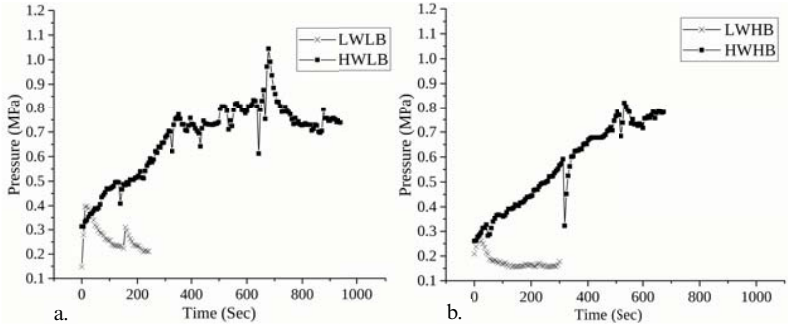

Figure 9. (a) Extrusion pressure of the low H_2O vs the high H_2O for the low binder paste. (b) Extrusion pressure of the low H_2O vs the high H_2O for the high binder paste.

GREEN STRENGTH RESULTS

Figure 10 below shows that the strength of high water extrudate is higher than the strength of low water extrudate. Previously as shown in Figure 9 that the extrusion pressure of the high water paste is higher and vice versa. The high binder extrudate has lower green strength comparing to low binder extrudate that will be discussed in a future paper.

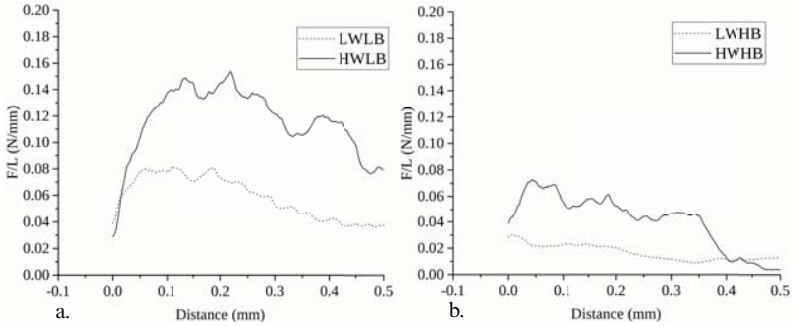

Figure 10. (a) The green strength of the low H_2O vs high H_2O for the low binder extrudate, (b) The green strength of the low H_2O vs high H_2O for the high binder extrudate.

GREEN MICROSTRUCTURE ANALYSIS

Figure 11 shows cross sections of low and high water extrudates. There are noticeable differences in the microstructure due to the water variations. The low water extrudates have cracks and uneven pores size comparing to the high water extrudate. These defects can impact the green strength of the extrudates as shown in Figure 10.

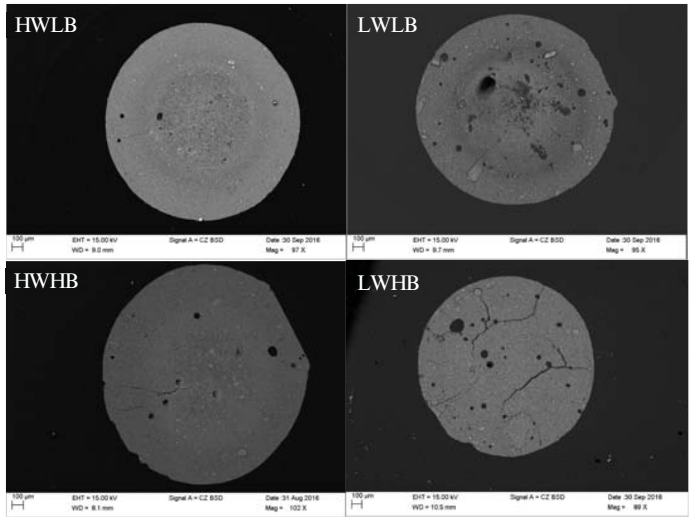

Figure 11. SEM images of the extrudate cross section of low and high water with the low binder (LWLB) and (HWLB), respectively. Also, the extrudate cross section of low and high water with high binder (LWHB) and (HWHB) binder, respectively at low magnification.

Figure 12 shows a fluctuation in the pores distribution from the edge toward the center of the extrudate cross section. Figure 12 (a), the low binder extrudate with low and high water shows there are a spatial variation, it seems that the porosity is lower near the center and the edge. However, in the high binder extrudates with high water content the porosity decreases toward the edge as shown in Figure 12 (b) The spatial variation might be due to the mixture composition as well as the extrusion parameters. Spatial variation could easily change the catalytic performance by having variable pore size distribution as shown in Figure 13.

In Figure 13, the high water extrudate with low or high binder content are densified when compared to the low water extrudate with low or high binder content. This could be due to the high extrusion pressure as shown before in Figure 9. The agglomerations size is larger in the case of the low water extrudate with low and high binder content as shown in Figure 13.

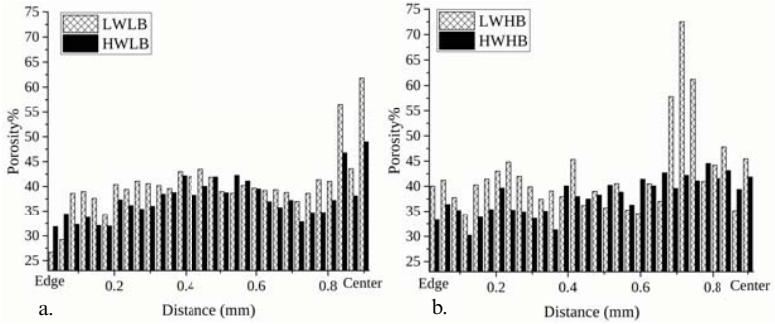

Figure 12. The distribution of porosity from the edge towards the center of extrudates as determined using the ImageJ software on infiltrated and polished sections. (a) Low H_2O vs high H_2O for the low binder extrudate, (b) Low H_2O vs high H_2O for the high binder extrudate

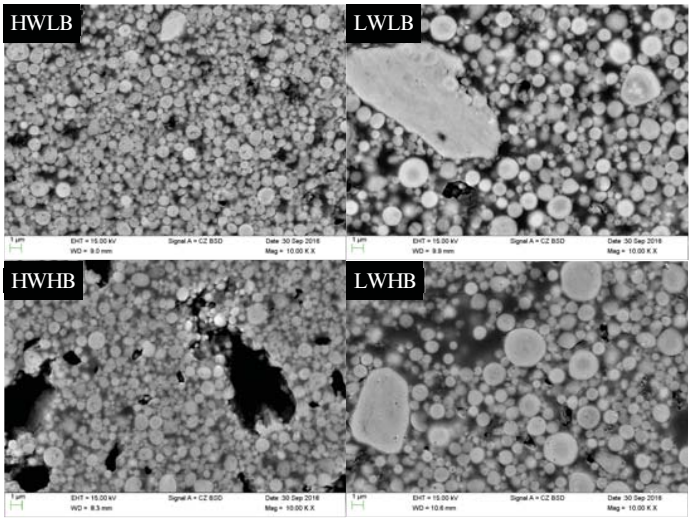

Figure 13. SEM images of (HWLB), (LWLB), (HWHB), and (LWHB) extrudates at 10000x magnification.

CONCLUSIONS

This study showed that there is a correlation between torque rheometry and capillary rheometry analyses, green strength, and green microstructure for titania pastes and extrudates varying water content. The high water content pastes/ extrudates with low or high binder content shows a lower mixing torque and a shorter time to achieve the steady state. The extrusion pressure increases as the water content increases. The high water content can result in improved green strength of extrudate.

The water content factor can be caused a microstructural variability. The microdefects are lowered using a high water content. There are variations in the porosity distribution and densification due to varying water content, with lower water content pastes/ extrudates commonly being more porous.

ACKNOWLEDGMENTS

This research was sponsored by the National Science Foundation I/UCRC Award No.1540027. The views and conclusions contained in this document are those of the authors and should not be interpreted as representing the official policies, either expressed or implied, of the National Science Foundation or the U.S. Government. The U.S. Government is authorized to reproduce and distribute reprints for Government purposes notwithstanding any copyright notation herein.

Thank you for the undergraduate assistants Priya Shah and Frank Maniaci for their help in performing various experiments and tasks. Dr. Sukanya Murali for her help in the SEM training and her expertise in image analysis. Joe Prati for the TGA experiment. Eric Bennett, John Casola, and Chuck Rohn (Malvern Instruments Ltd.) for the equipment and help in this research. Sara Reynaud for programming the Kinexus sequence. Ian Maher for his help in the moisture measurement.

REFERENCES

[1]Benbow, J., & Bridgwater, J. (1993). Paste flow and extrusion. Oxford: Clarendon Press.

[2]Chevalier, L., Hammond, E., & Poitou, A. (1997). Extrusion of TiO_2 ceramic powder paste. Journal of materials processing technology, 72(2), 243-248.

[3]Bagheri, S., Muhd Julkapli, N., & Bee Abd Hamid, S. (2014). Titanium dioxide as a catalyst support in heterogeneous catalysis. The Scientific World Journal, 2014.

[4]Rough, S. L., Bridgwater, J., & Wilson, D. I. (2000). Effects of liquid phase migration on extrusion of microcrystalline cellulose pastes. International journal of pharmaceutics, 204(1), 117-126.

[5]Guilherme, P., Ribeiro, M. J., & Labrincha, J. A. (2013). Behaviour of different industrial ceramic pastes in extrusion process. Advances in Applied Ceramics.

[6]Cheng, B., Zhou, C., Yu, W., & Sun, X. (2001). Evaluation of rheological parameters of polymer melts in torque rheometers. Polymer Testing, 20(7), 811-818.

[7]August, C. R., & Haber, R. A. (2009). Benbow analysis of extruded alumina pastes. Whitewares and Materials: Ceramic Engineering and Science Proceedings, Volume 25, (2), 15.

[8]Majidi, S., Motlagh, G. H., Bahramian, B., Kaffashi, B., Nojoumi, S. A., & Haririan, I. (2013). Rheological evaluation of wet masses for the preparation of pharmaceutical pellets by capillary and rotational rheometers. Pharmaceutical development and technology, 18(1), 112-120.

[9]Supati, R., Loh, N. H., Khor, K. A., & Tor, S. B. (2000). Mixing and characterization of feedstock for powder injection molding. Materials Letters, 46(2), 109-114.

[10]Suri, P., Atre, S. V., German, R. M., & de Souza, J. P. (2003). Effect of mixing on the rheology and particle characteristics of tungsten-based powder injection molding feedstock. Materials Science and Engineering: A, 356(1), 337-344.

[11]Rough, S. L., Wilson, D. I., & Bridgwater, J. (2002). A model describing liquid phase migration within an extruding microcrystalline cellulose paste. Chemical Engineering Research and Design, 80(7), 701-714.

[12]ASTM D6175-03(2013) Standard Test Method for Radial Crush Strength of Extruded Catalyst and Catalyst Carrier Particles, ASTM International, West Conshohocken, PA, 2013, https://doi.org/10.1520/D6175-03R13.

[13]Ku, N. (2015). Evaluation of the behavior of ceramic powders under mechanical vibration and its effect on the mechanics of auto-granulation (Doctoral dissertation, Rutgers University-Graduate School-New Brunswick).

COMPACTION PLASTICITY OF SPRAY DRIED ALUMINA GRANULES TO FORM MICROSTRUCTURAL UNIFORMITY AND GREEN STRENGTH

I. P. Maher, R. A. Haber
Department of Materials Science and Engineering, Rutgers University, Piscataway, N.J. 08854

ABSTRACT

Microstructural variability in ceramic green bodies has been a continuing issue during ceramic processing as it can lead to unwanted pores and fractures developing in the microstructure. Moisture and binders within the granules are needed to create temporary adhesion and strength before the firing process. The moisture governs the mechanical properties of the binder and thus affects the compaction behavior of the granules and the microstructure of the green body. In this study, alumina was the system analyzed and will be processed through thermal spray drying. The plasticity of the spray dried granules on a compaction scale is used as a tool to determine the effects of binder and characteristics within the slurry prior to spray drying have on the compaction behavior of the granules. Image analysis of compacted samples will be conducted to understand and determine what affects the microstructural uniformity and green strength of the compacted ceramic.

INTRODUCTION

In the ceramic industry, failures during production due to microstructural defects, or fractures cause losses at a production standpoint. One mechanism that can cause fractures is inadequate cohesion of the granules when pressing [1]. Moisture and binders within the granules are needed to create temporary adhesion and strength during the pressing stage and prior to the sintering process. The compaction behavior of the granules strongly depends on the characteristics and properties of the granules and binder [2]. With little to no binder and very low moisture content, there would be minimal adhesion of the particles while packing, thus creating a weak ceramic green body [1, 2]. While compacting, granules with little to no moisture can cause fractures where pores are located within the microstructure [2, 3]. During the sintering stage these fractures can lead to variations in localized green bulk density. Granules that contain moisture for adequate adhesion however, soften the granules and contribute to forming microstructural uniformity within the compacted green body [2, 3]. The moisture of the ceramic granules strongly affects the properties of the green body ceramic [2, 3]. The moisture even governs the mechanical properties of the binder and thus affects the compaction behavior of the granules and the microstructures of the ceramic green body [2, 3]. Minimizing these defects and failures in the processing stage is the focus of this study and proves a need in the ceramic industry. Determining the processing roles that may lead to microstructural uniformity such as binders, slurry characteristics before spray drying, and pressing conditions, will help narrow the problem of microstructural variability within ceramic processing.

Alumina (Al_2O_3), was the model system chosen for this study due to wide applicability in the technical ceramic industry [4]. Spray drying is the most widely used granulation technique for pressed alumina and will be the technique used for this study. Alumina granules will be compacted to understand the different compaction behavior of alumina granules with varying process differences prior to spray drying. The processing roles that will be studied include the viscosity of the slurry, the percentage of binder within the slurry, and the spray dried granule size distribution during compaction analysis. Samples will be pressed at various pressures to conduct image analysis, using a scanning electron microscope, in attempt to visualize microstructural variations that occur with varied processing changes prior to spray drying. The techniques used to image a compacter green ceramic sample were determined from previous studies within the research group

at Rutgers' University. Microstructural imaging will be used as a tool to visualize the compaction behavior of the spray dried granules as well as performing mechanical analysis of the compaction behavior.

EXPERIMENTAL APPROACH

Alumina slurries were processed and milled for 24 hours [5, 6]. The alumina powder used in the slurry was A16 alumina from Almatis Incorporated (Almatis Inc. – Leetsdale, PA.). The binders used in the slurry were polyethylene-glycol (PEG) and polyvinyl-alcohol (PVA). The PEG used was PEG 300 from Acros Organics (Acros Organics – ThermoFisher Scientific, Waltham, MA.) and the PVA used was a 20% aqueous solution prepared by SELVOL (SELVOL E 205 PVA) and distributed by Sekisui (Sekisui – Secaucus, N.J.). The dispersant used in the slurry was sodium polyacrylate (ACUMER 9400). Different percentages of the PVA binder were added at 0.75% and 1.5% on the total slurry weight and 1.35% and 2.7% based on the solids weight within the slurry [5, 6]. The PEG 300 was kept constant in all slurries at 0.15% based on the solids weight and acted solely as a plasticizer for the slurry. The slurries were milled for 23 hours followed by adding more dispersant in the final milling hour to drop the viscosity prior to spray drying [5, 6]. The initial percentage of dispersant added for the first 23 hours was 0.3% based on the solids weight within the slurry. The additional percentage of dispersant added within the last hour of milling varied and depended on the percentage of PVA in the system and on what was the desired viscosity range of the slurry prior to spray drying. Dispersant added was based on volumetric amounts of a 50% of ACUMER 9400 and 50% deionized water. Different viscosities were examined prior to spray drying to determine if there was a difference in the compaction behavior of the spray dried granules since the characteristics of the granules depend on the process parameters and slurry characteristics before spray drying [7].

The spray dryer used for this study was a Niro Atomizer Minor Plant with a fountain nozzle (Niro – GEA, Columbia, MD.). The slurries were pumped into the nozzle at a constant speed and atomized into the drying chamber at a pressure of 30 psi. The inlet temperature of the spray dryer was set to 150˚C with the outlet ranging from 60-70˚C [1, 8]. The spray dried granules was then screened through varied sized sieves to evaluate particle size analysis on the spray dried granules. The moisture of the spray dried granules varied from 0.5-1.0% moisture therefore no further heat treatment was needed to be conducted to ensure the mechanical properties of the organic binder were governed during the compaction of the granules.

Compaction analysis was also conducted to determine the compaction behavior of the granules. An Instron tensile and compressive tester was used to perform the compaction curve analysis up to a force of 20 kN with a 13 mm diameter die (Instron – Norwood, MA.). The compaction rate used on the Instron was 0.5 mm per minute. The Instron instrument returns the displacement change during the test and the respective force measurement. From this data, density and pressure can be calculated and plotted as shown below in Figure 1a to determine the three stages of compaction. Stage one is where granules flow and rearrange, stage two is where granules begin to deform, and stage three is where granules begin to densify and join [9]. A schematic of the compaction die used is shown below in Figure 1b.